The Influence of Meltwater on Phytoplankton Blooms Near the Sea-Ice Edge

C. W. Lester[1,2], T. J. W. Wagner[1], Dylan E. McNamara[1], M.R. Cape[3]

[1]Department of Physics and Physical Oceanography/Center for Marine Science, University of North Carolina Wilmington, Wilmington, NC, United States
[2]Division of Earth and Ocean Sciences, Nicholas School of the Environment, Duke University, Durham, NC, United States
[3]Applied Physics Laboratory, University of Washington, Seattle, WA, United States

Key Points:

- Observations show that sea-ice edge phytoplankton concentrations are spatially correlated with sea-ice meltwater.
- We present an idealized model of phytoplankton dynamics where the influence of meltwater and sunlight is parameterized in phytoplankton growth and death rates.
- Model output captures key characteristics of observed phytoplankton blooms in Fram Strait, highlighting the role of meltwater in bloom development.

Corresponding author: C. W. Lester, `conner.lester@duke.edu`

Abstract

Phytoplankton blooms occur annually at the sea-ice edge throughout the Arctic during the spring melt period. Our study considers how these spring blooms may depend on sea-ice meltwater, focusing on the role of horizontal mixing and advection. We extend the classic Fisher reaction-diffusion equation to consider a time- and space-varying death rate that represents the role of meltwater in the system. Our results indicate that blooms peak at a characteristic distance from the ice edge where *(i)* meltwater is concentrated enough to stratify the upper ocean such that the phytoplankton are confined near the surface and *(ii)* phytoplankton have been exposed to sufficient sunlight to allow for optimized growth. The results reproduce key characteristics of a large bloom observed in Fram Strait in May 2019. Our findings support the idea that sea-ice meltwater is of central importance in setting the spatial patterns of Arctic phytoplankton blooms.

Plain Language Summary

In the Arctic, each spring the appearance of the sun awakens the region's ecosystem. In particular, the blooming of phytoplankton – which form the base of the Arctic marine food web — is an early phenomenon that depends on the availability of sunlight. In this study we present a model that supports the idea that sunlight alone is not enough to drive large plankton blooms in the open ocean: an influx from sea-ice meltwater is also needed. This meltwater (which is fresh and light) acts to maintain an ocean surface layer that is thin and separated from the ocean below. The plankton are confined to this surface layer where they can absorb plentiful sunlight and grow into large blooms. Our model sheds light on this central role of sea-ice meltwater for the growth of Arctic phytoplankton.

1 Introduction

Springtime in the Arctic Ocean is marked by large-scale algal growth events, known as phytoplankton blooms. Phytoplankton form the base of the trophic food web and their blooming constitutes a key phenomenon in the seasonal cycle of the Arctic ecosystem (Wassmann & Reigstad, 2011; Behrenfeld & Boss, 2014; Leu et al., 2015). Algae blooms also impact ocean-atmosphere dynamics through primary production and associated carbon dioxide uptake (Wassmann & Reigstad, 2011).

In certain regions of the Arctic there has been a recent increase in the intensity of phytoplankton blooms (Lewis et al., 2020). Cherkasheva et al. (2014) have found that this increase is particularly notable near the sea-ice edge. During typical winter-spring transitions, the sympagic environment of the sea-ice edge is populated by algae communities that, under favorable conditions, grow rapidly into blooms (Leu et al., 2015). Central factors in determining the magnitude and spread of these blooms are the availability of nutrients and sunlight, and the stratification of the upper ocean. In the spring, increasing solar irradiance in the Arctic not only provides sunlight for photosynthesis, but also drives melting of sea ice. Although meltwater is typically nutritionally sparse, it creates a stably stratified ocean surface layer that constrains phytoplankton in the euphotic zone, making it a key factor in bloom development (Waniek et al., 2005; Cherkasheva et al., 2014; Janout et al., 2016; Mayot et al., 2018, 2020).

The link between meltwater and algae blooms is illustrated by Landsat 8 satellite imagery which shows strong spatial correlations between phytoplankton concentrations and low sea surface temperatures near, or below, 0°C (Figure 1) – an indicator for high meltwater concentrations. Concerns about future changes in the sea-ice cover and its role in altering spring bloom dynamics have further motivated recent field efforts (Cherkasheva et al., 2014; Arrigo & van Dijken, 2015). Although such observational work and the satellite images of Figure 1 suggest a dynamic relation between phytoplankton blooms and

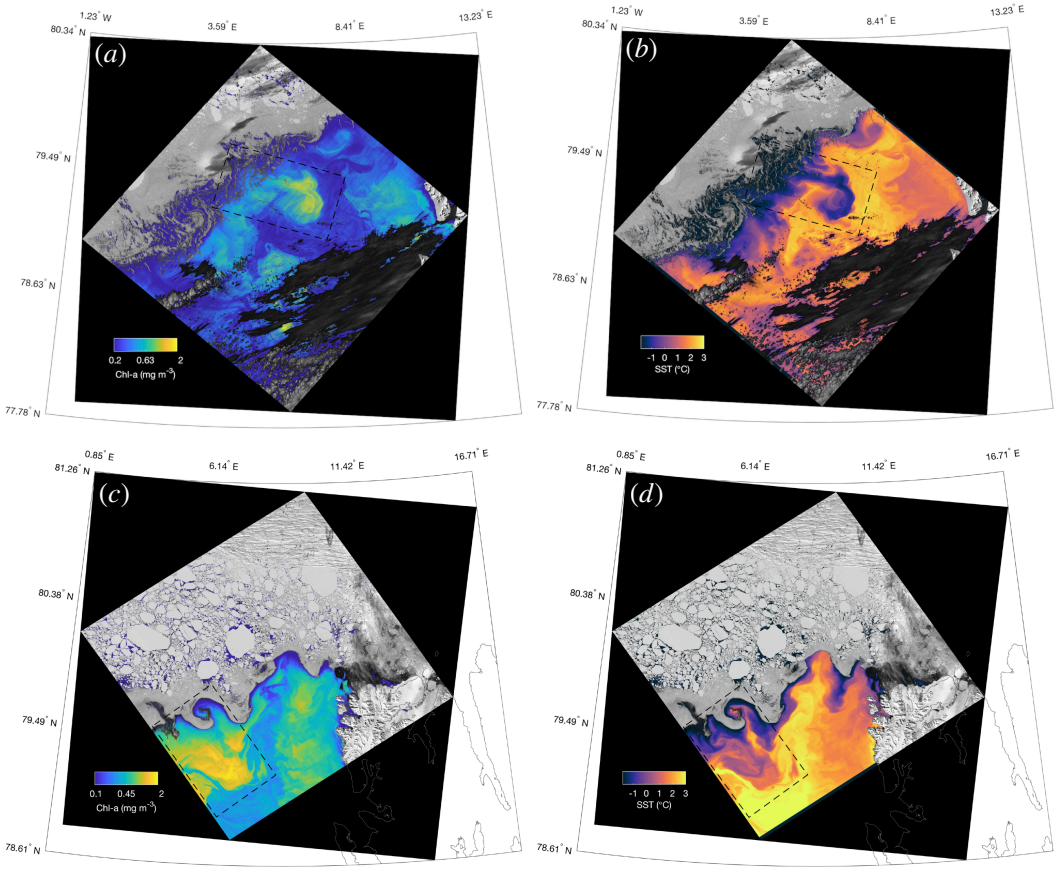

Figure 1. Landsat 8 images of an evolving ice-edge phytoplankton bloom taken in Fram Strait (sea ice is shown in grey/white). Svalbard is seen in the far right of both images. Left column (a,c) shows chlorophyll-a (mg m^{-3}), right column (b,d) SST (°C). Top (a,b): May 26, 2019. Bottom (c,d): May 30, 2019. Bloom regions used in the data analysis (see text) are outlined by dashed boxes.

sea-ice melt, our understanding of the role meltwater plays in sea-ice edge phytoplankton blooms remains incomplete.

Most research to date on this topic has aimed at resolving the vertical processes that govern stratification–bloom interactions, often using one-dimensional single column models (A. Taylor, 1988; Jin et al., 2007; Mellard et al., 2011). Previous studies have found that phytoplankton blooms occur when the surface mixed layer shoals to a critical depth in the spring (Sverdrup, 1953), when turbulent mixing is insufficient to remove the plankton from the surface (Huisman et al., 1999), or when the balance between phytoplankton division and grazer consumption is perturbed (Behrenfeld & Boss, 2014). Stratification of the upper ocean due to meltwater from sea ice may therefore play a central role in determining whether a bloom is initiated and how large it will grow. This hypothesis is supported by anecdotal observational evidence of striking correlations between blooms and meltwater, as discussed above. However, while vertical processes have been studied in some detail, the influence of horizontal mixing and advection of meltwater on early bloom development and the resulting spatial characteristics of ice-edge blooms have received less attention.

Previous efforts to model horizontal distributions of spring blooms in the open ocean invoke mechanisms that drive stratification through eddy (Omand et al., 2015; Mahadevan et al., 2012) or ocean-front (J. R. Taylor & Ferrari, 2011) formations. In a similar vein, here we model horizontal features of spring blooms near the sea-ice edge that arise due to the stratifying effects of meltwater input. Namely, we present an idealized model that accounts for phytoplankton death and growth rates in a way that is physically motivated by the ice-edge environment during the spring melt period. The model builds on previous work using the Fisher reaction-diffusion equation as a representation of open-ocean plankton dynamics (Birch et al., 2007). Specifically, we parameterize the role of meltwater and associated surface stratification which retains phytoplankton in the euphotic zone and thus provides enhanced growing conditions near the ice edge.

2 Plankton Model

Birch et al. (2007) simulated phytoplankton dynamics using the Fisher equation (Fisher, 1937; Kolmogorov et al., 1937) with a spatially variable growth rate and an incompressible velocity field:

$$P_t + \mathbf{u} \cdot \nabla P = \gamma(\mathbf{x})P - \nu P^2 + \kappa \nabla^2 P, \tag{1}$$

where $P(\mathbf{x}, t)$ is phytoplankton concentration, $\mathbf{u}$ is the velocity field, $\gamma(\mathbf{x})$ is a spatially variable growth rate, ν is a constant death rate, and κ is a constant diffusivity.

Birch et al. (2007) present equation (1) in the context of open-ocean plankton dynamics with the goal of deriving bounds on total plankton biomass. The model as presented by Birch et al. (2007) has no explicit dependencies on nutrient limitations or predation. Nonetheless, plankton are able to reach a nontrivial steady state with rich transient dynamics dependent on stirring magnitude $|\mathbf{u}|$ and diffusivity κ.

Here, we modify equation (1) to study the dependence of phytoplankton blooms on meltwater near a sea-ice edge. To simulate phytoplankton-meltwater dynamics we include space and time dependence for the death rate ν in equation (1). Our hypothesis is that ν broadly reflects the effects that meltwater has on phytoplankton bloom development, namely that when meltwater is concentrated the death rate is lowered as phytoplankton are kept near the surface. The phytoplankton growth rate γ is broadly dependent on sunlight availability, nutrient abundance and predation, and is typically a function of space and time as well.

Beyond the central role of the mixed layer, bloom dynamics are controlled by nutrient availability and grazing pressure from zooplankton (Truscott & Brindley, 1994; Huppert et al., 2002; Behrenfeld & Boss, 2014). We note that blooms near the marginal ice zone may not be nutrient limited in the early spring as recent winter ice growth and associated salt rejection drive vertical convection and upward-mixing of nutrients from depth (Mayot et al., 2018). Here, we are primarily interested in the dynamical effects that horizontal mixing and advection of meltwater have on the evolution of blooms. In order to isolate these effects, we take other factors impacting the system, such as nutrient and light availability and grazing pressure, to be fixed. This can be approximated by taking the growth rate γ to be constant. Since we are focusing on the early stages of the bloom, the assumption that the system is not nutrient limited appears justified. Similarly, since we are considering a time-scale of only a few days near the initiation of the bloom, sunlight availability can be assumed to be approximately constant.

With these modifications to equation (1), the model takes the form:

$$P_t + \mathbf{u} \cdot \boldsymbol{\nabla} P = \gamma P - \nu(\mathbf{x}, t)P^2 + \kappa \nabla^2 P, \tag{2}$$

$$\nu_t + \mathbf{u} \cdot \boldsymbol{\nabla} \nu = \alpha \nu + \kappa \nabla^2 \nu. \tag{3}$$

Equation (2) is equivalent to (1) aside from γ now being constant and $\nu(\mathbf{x}, t)$ varying in space and time (γ and ν only take positive values). Note that equation (2) and (3)

contain the same velocity field $\mathbf{u}$ and diffusivity κ. This presupposes that phytoplankton are passive tracers which are advected and diffused at the same rate as the surface water in which they reside. The term $\alpha\nu$ in equation (3) causes exponential growth of ν (α being a positive constant). When ν reaches an upper bound ν_{max}, we set $\alpha = 0$. The constant ν_{max} is interpreted as the open-ocean background death rate (when there is no meltwater). The term $\alpha\nu$ can be interpreted as a proxy for wind-driven vertical mixing, where vertical mixing is suppressed near the ice edge and increases as you move toward open water. From here forward we will refer to α as the vertical mixing rate.

We take the velocity field $\mathbf{u} = (u, v)$ to be the stochastic two-dimensional field used by Birch et al. (2007), with slight modifications to mimic stirring at an ideal sea-ice edge:

$$\mathbf{u}(\mathbf{x}, t) = \begin{cases} U(c + (1-c)cos(k_m y + \phi_x),\ 0) & \text{for } n\tau \le t < (n+1/2)\tau, \\ U(c,\ cos(k_m x + \phi_y)) & \text{for } (n+1/2)\tau \le t < (n+1)\tau, \end{cases} \tag{4}$$

where $(x, y) \in [0, \ell)$. The piecewise velocity field alternates on a given decorrelation time period τ with an imposed constant advection away from the ice edge of magnitude cU, such that space-time averages are $\langle u \rangle = cU$ and $\langle v \rangle = 0$. The positive constant c is added to insure mean advection away from the ice edge boundary; the wave number $k_m = 2\pi m/\ell$, where ℓ is the domain length scale; and ϕ_i is a phase shift randomly chosen between 0 and 2π each period.

Boundary conditions are applied to equations (2) and (3) that reflect sea-ice meltwater and phytoplankton conditions at and near the sea-ice edge at the beginning of the melt season. At the ice edge ($x = 0$), we supply the domain with a constant influx of low death rate (ν_0) and low phytoplankton concentration (P_0). This influx is balanced by an equally constant outflux at $x = \ell$. The domain is thus non-periodic in x. The perpendicular boundaries are periodic at $y = (0, \ell)$. A snapshot of a typical spun-up model state is seen in Figure 2. We initialize the model with the uniform background density $P = P_0$ and maximum death rate ν_{max} (i.e., no meltwater). In all simulations, $c = 0.5$, $m = 1$, and $\nu_{max} = 20\nu_0$. After several time steps a bloom develops near the influx boundary, the magnitude of which is bounded by the carrying capacity $K = \gamma/\nu_0$.

The model is characterized by three dimensionless parameters: *(i)* The Péclet number – the ratio of the diffusive time scale ℓ^2/κ to the advective time scale ℓ/U: Pe$\equiv U\ell/\kappa$;

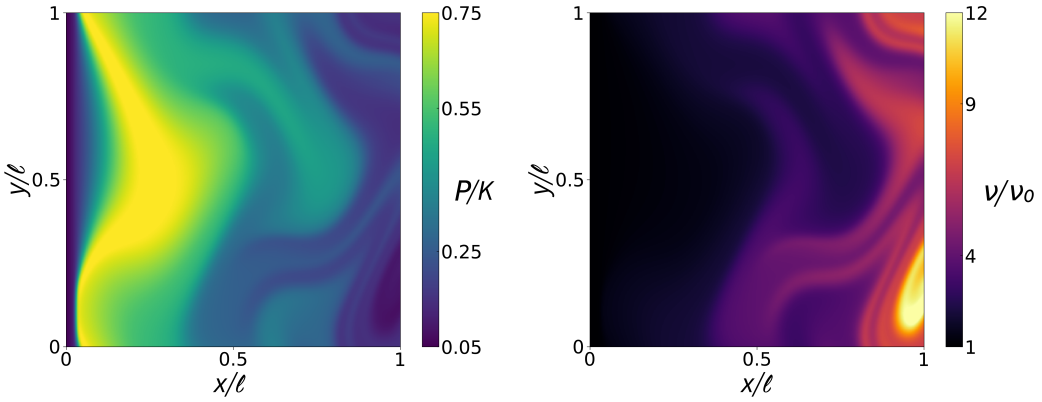

Figure 2. Snapshot of converged model state. Shown are phytoplankton concentration P rescaled by the carrying capacity K (left) and death rate ν rescaled by ν_0 (right). Here, Da = 20, $\alpha/\gamma = 0.05$, and $k = 5 \times 10^{-6}$.

(ii) The Damköhler number – the ratio of the advective time scale to the biological growth time scale: $\mathrm{Da} \equiv \gamma\ell/U$; *(iii)* The ratio α/γ of the vertical mixing rate α and growth rate γ. For the following analysis it is convenient to further define the characteristic diffusivity $k \equiv 1/(\mathrm{Da}\,\mathrm{Pe}) = \kappa/\gamma\ell^2$.

2.1 Limit of no horizontal diffusion

Here, we consider environmental conditions where diffusive time scales are much larger than advection time scales ($\mathrm{Pe} \to \infty$). To explore this limit we set $\kappa = 0$ in equations (2) and (3). In this case, we can readily solve for the steady-state plankton concentration for a given advective field. Considering the idealized flow field $\mathbf{u} = \langle\mathbf{u}\rangle/c = (U, 0)$, the zero-diffusion equivalents of equations (2) and (3) can be written as:

$$U\frac{dP}{dx} = \gamma P - \nu P^2, \tag{5}$$

$$U\frac{d\nu}{dx} = \alpha\nu. \tag{6}$$

This is solved to give plankton concentration as a function of distance from the ice edge x:

$$P(x) = \frac{e^{\frac{\gamma x}{U}}}{\frac{\nu_0}{\gamma+\alpha}(e^{\frac{x}{U}(\gamma+\alpha)} - 1) + \frac{1}{P_0}}. \tag{7}$$

Here, no bound is imposed on ν (i.e., $\alpha = 0$ for $\nu = \nu_{max}$ no longer applies) and $P \to 0$ as $\nu, x \to \infty$. This can be interpreted as the open-ocean background concentration of phytoplankton being zero.

The solution $P(x)$ in equation (7) highlights the spatial dynamics that may be expected of a bloom in this idealized environment. Namely, $P(x)$ has the intuitive shape of a heavy tailed distribution, where phytoplankton grow rapidly from a small initial value close to the ice edge boundary, peak, and decay slowly away from the ice edge. This "bloom curve" is sensitive to the parameters α/γ and Da (Figure 3a,b). For instance, as the ratio of vertical mixing to phytoplankton growth rate (α/γ) gets larger the death rate increases more quickly with x, which reduces the bloom magnitude and spread (Figure 3a). This can be interpreted as larger vertical mixing rates destabilizing and mixing the surface waters more efficiently, resulting in a less intense bloom. And as the ratio of the biological growth versus advective time scales (Da) decreases the bloom grows spatially, spanning a larger range in x, and its peak P_{max} is pushed further from the $x = 0$ boundary (Figure 3b). That is, a large influx of meltwater from the ice edge allows for a spatially large bloom to occur, peaking at a greater distance from the ice edge because of the increased advection speed.

3 Phytoplankton Meltwater Dependence

Equation (7) provides insight into the spatial behavior of an ice edge bloom subject to an idealized velocity field. However, real-world phytoplankton blooms are subject to highly variable horizontal velocities, resulting in large fluctuations of phytoplankton concentration with distance from the ice edge (Figure 1). Since $P(x)$ depends explicitly on the velocity field $\mathbf{u}$, a comparison between model output and observations (where $\mathbf{u}$ is not known) is made difficult. However, since the advection rates for P and ν are the same in equations (2) and (3), we can obtain a solution $P(\nu)$, for negligible diffusion, that is invariant of $\mathbf{u}$:

$$P(\nu) = \frac{\nu^{\frac{\gamma}{\alpha}}}{\frac{1}{\gamma+\alpha}(\nu^{\frac{\gamma}{\alpha}+1} - \nu_0^{\frac{\gamma}{\alpha}+1}) + \frac{\nu_0^{\frac{\gamma}{\alpha}}}{P_0}}. \tag{8}$$

This solution represents the phytoplankton concentration as a function of death rate (meltwater) and produces similar shaped bloom curves as $P(x)$ (Figure 3c,d). The velocity

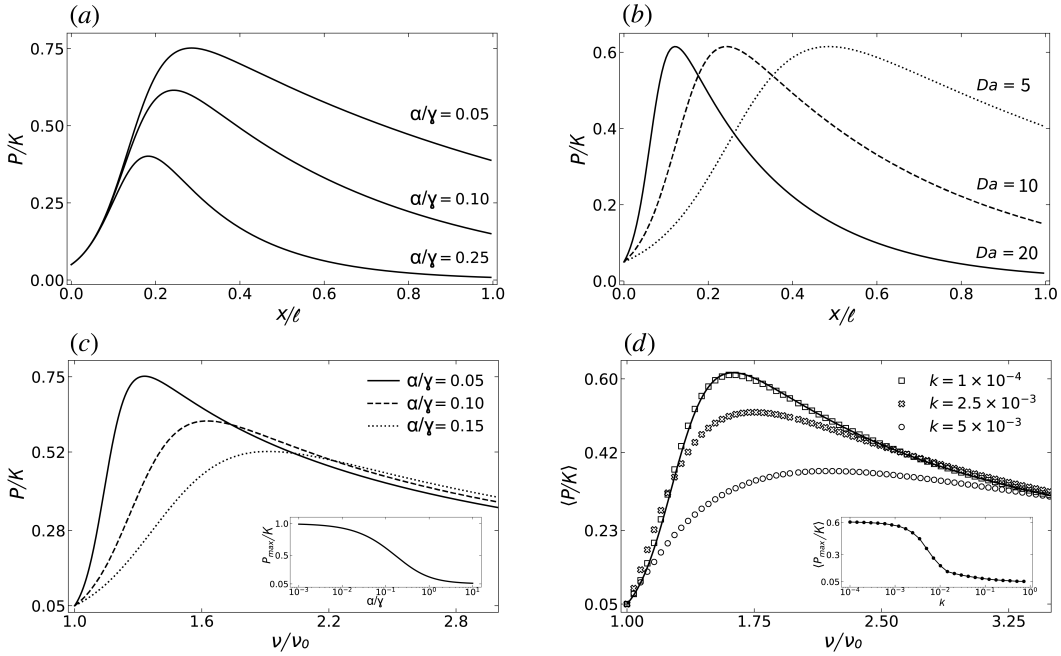

Figure 3. Top row: Rescaled phytoplankton concentration as a function of distance from the ice edge $P(x)$ on model parameters. (a) Analytic solutions of $P(x)$ for different values of α/γ. Here, Da $=$ 10. (b) Analytic solutions of $P(x)$ with varying Da. Here, $\alpha/\gamma = 0.1$. Bottom row: Rescaled phytoplankton concentration as a function of rescaled death rate $P(\nu)$. (c) Analytic solutions of $P(\nu)$ in the limit of no diffusion (equation 8), for different values of the characteristic growth rate α/γ. Inset: dependence of peak bloom value P_{max} on α/γ, with $P_{max} \rightarrow K$ as $\alpha/\gamma \rightarrow 0$ and $P_{max} \rightarrow P_0$ as $\alpha/\gamma \rightarrow \infty$. (d) Numerical steady state solutions for the full model (equations 2 and 3), for different values of dimensionless diffusivity k. Solutions found by binning ν and averaging the P values in each bin, represented by $\langle P \rangle$. The analytic solution for $k = 0$ (equation 8) is shown as the solid black line. Inset: P_{max} as a function of k, approaching P_0 as $k \rightarrow \infty$. Here, $\alpha/\gamma = 0.1$.

invariance of $P(\nu)$ is due to our initial assumption that phytoplankton are passive tracers and are advected at the same rate as the meltwater they reside in. Without the explicit dependence on horizontal motion, $P(\nu)$ allows us to qualitatively compare our model results to observational data (see below).

$P(\nu)$ is controlled by the parameter α/γ (Figure 3c). When α/γ is small (i.e., when vertical mixing is low or growth rate is high) the phytoplankton maximum P_{max} is large at low values of ν. In the limit $\alpha/\gamma \rightarrow 0$ the death rate becomes spatially constant at ν_0, allowing the bloom to reach full carrying capacity, with $P_{max} \rightarrow K$. When α/γ is large (i.e., when vertical mixing is high or growth rate is low) $\nu(P_{max})$ is pushed towards high values of ν and P_{max} is reduced, approaching the background concentration P_0 everywhere in the limit $\alpha/\gamma \rightarrow \infty$.

To explore the influence of non-zero horizontal diffusion on the phytoplankton concentration we numerically solve equations (2) and (3) with varying values of κ (Figure 3d). As expected, as diffusivity κ increases the bloom peak P_{max} is suppressed. In the limit $\kappa \rightarrow \infty$ the bloom peak vanishes and the plankton population in the domain homogenizes at P_0. In the limit $\kappa \rightarrow 0$, on the other hand, the plankton bloom follows the zero-diffusivity curve described by the analytic solution above (equation 8).

We note that equation (3) models the death rate as exponentially increasing with time and space. This gives rise to the asymptotic decay in the phytoplankton concentration as ν grows large (Figure 3c,d). Qualitatively similar shapes for $P(\nu)$ to those in Figure 3 are found if the death rate ν increases in any fashion with $\boldsymbol{x}, t$. That is, the bloom curve $P(\nu)$ does not change its qualitative shape as long as equation (3) has the form: $\frac{D\nu}{Dt} = f(\nu)$, with the conditions that $f(\nu) \geq 0$ and $f(\nu) = 0$ iff $\nu > \nu(P_{max})$.

Therefore, the exponential growth of equation (3), $\frac{D\nu}{Dt} = \alpha\nu$, represents just one possible functional form that is compatible with the observational data (see below). The physical interpretation here is that sea-ice meltwater is increasingly vertically mixed out of the surface layer with time and distance from the ice edge; the exact spatiotemporal dependence of this mixing however is beyond the scope of this study.

3.1 Comparison to Observations

The modeled $P(\nu)$ (equation 8, Figure 3c,d) suggests a dynamical interpretation of observed ice edge blooms (Figure 1). Because $P(\nu)$ is not dependent on the horizontal stirring scheme (and weakly dependent on diffusion; Figure 3d) it provides a simple framework for us to interpret key bloom characteristics that may be present in bloom data – characteristics we may expect to be approximately independent of horizontal stirring as well.

The scenes in Figure 1 are from high spatial resolution (30m) satellite imagery, taken May 26 and 30, 2019, by the NASA/USGS Landsat 8 mission in the Arctic region of Fram Strait. This imagery captures horizontal ocean surface data from the top several meters of the water column. We consider sea-surface temperature (SST) and chlorophyll-a (chl-a) as rough proxies for sea-surface meltwater and phytoplankton concentrations, respectively. Namely, low values of SST correspond to high meltwater concentration (low ν) and high values of chl-a to high phytoplankton concentration (high P).

To get at the relationship between phytoplankton and meltwater in the satellite data we compute binned averages of chl-a as a function of SST for the main bloom regions in Figure 1 (outlined by dashed boxes). The results reveal two distinct regimes, present in both scenes: a positive correlation for low SST and a negative correlation for higher SST (Figure 4). In regions where SST is low and meltwater concentration is high the positive correlation between chl-a and SST suggests that in this region the algae grow as they are transported away from the ice edge. In regions where SST is high (i.e., low meltwater concentration) the negative correlation between chl-a and SST suggests that the growth-favoring stratification is lost as meltwater is mixed vertically, and algae levels drop to a background value of chl-a present in the open ocean.

Note that both curves in Figure 4 show similar mean chl-a concentrations ($\langle$chl-a$\rangle \approx 0.4\mathrm{mg\,m^{-3}}$) at low SST ($\approx -1.8°\mathrm{C}$) near the ice edge. This suggests a relatively unchanged level of algae near the sea ice between May 26 and May 30. Similarly, the chl-a levels in the warm water limits are comparable for the two scenes ($\langle$chl-a$\rangle \approx 0.25 - 0.3\mathrm{mg\,m^{-3}}$), indicating that this may be a background level of algae in the region during this period.

Because both scenes were collected in the same region only four days apart it is reasonable to assume that they represent different stages of the same bloom event. The earlier date (Figure 4, blue) shows the earlier, less developed stage while the later date (red) shows the more developed stage at which point the peak chl-a value has roughly doubled. The earlier scene exhibits its highest chl-a in rather cold waters (SST$\approx -1°\mathrm{C}$) near the ice edge and an approximately linear increase of chl-a from the ice edge to this peak. As the bloom grows more mature, the positive correlation between meltwater and chl-a extends to SST$\approx 0°\mathrm{C}$, which suggests that conditions are more advantageous for algae growth with increasing distance from the ice edge up to waters with $0°\mathrm{C}$. One ex-

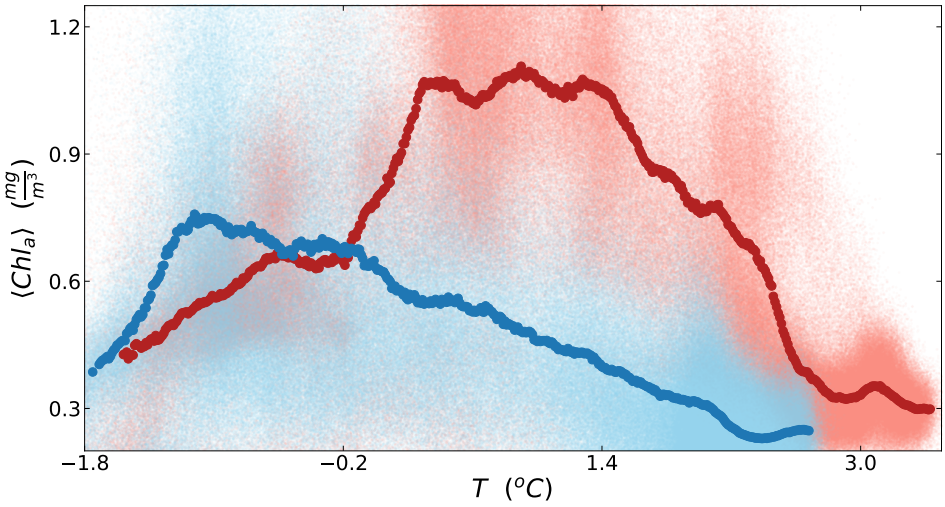

Figure 4. Observed chl-a versus SST from the regions outlined in Figure 1 (dashed boxes). Here, May 26 data is shown in blue and May 30 data in red. The large dots show averages of chl-a in SST bins (600 bins with width 0.01°C). Also plotted are 10^6 randomly selected pixels from each scene (blue and red point clouds). We ignore values of chl-a < 0.16 mg m^{-3} and > 4 mg m^{-3} and SST values < -1.8°C, which are likely satellite measurement anomalies. We note that the general shapes of the blue and red curves above are robust for different sized and oriented bounding boxes in Figure 1.

planation for this correlation is that the algae grow as they are advected away from the ice edge (by sub-mesoscale eddies, Figure 1) while confined to the meltwater-stratified shallow surface layer and exposed to an abundance of sunlight. The peak of the bloom therefore moves further into warmer waters and increases in maximum value.

The different slopes in the SST–chl-a relation for low SST ($< -.5$°C) between the two scenes may be (at least in part) due to differences in vertical mixing rates. A larger vertical mixing rate and weakened stratification in the later scene would explain the suppression of bloom growth (red curve), while the steeper slope for the earlier stage (blue curve) may indicate quiescent conditions with little vertical mixing and rapid algae growth.

At the later stage of the bloom, conditions appear to be optimized for 0 <SST< 1.4°C, where peak ⟨chl-a⟩ concentrations are approximately constant at ≈ 1 mg m^{-3}. We note that from MODIS data (NASA Goddard Space Flight Center, 2018 Reprocessing) we estimate this event to be the largest spring bloom in Fram Strait since MODIS started observing ocean surface color in 2002 (not shown).

For SST values higher than those at the chl-a peaks, we observe roughly linear decreases in chl-a in both cases which level off at $\approx 0.25{-}0.3$ mg m^{-3}. This may be due to a loss of stratification with decreasing meltwater concentration in the surface layer. The steeper slope of the later stage may again indicate enhanced vertical mixing during that period.

The satellite-derived chl-a curves share similarities with major features in the model of $P(\nu)$ above (Figure 3c,d). As a bloom evolves in the model there is an initial growth phase at low ν associated with the influx of low phytoplankton concentration P_0 and low death rate ν_0 into the domain. This is analogous to the low chl-a and low SST values near the ice edge as seen in the data (Figures 1 and 4), where low SST indicates a meltwater-stratified shallow surface layer, associated with low phytoplankton death rate. Away from

the model influx boundary, P and ν grow according to their respective growth rates, γ and α. In regions of high ν, the plankton concentration decays towards a steady-state value, the background plankton concentration. At an early stage of bloom evolution the bloom peak P_{max} is small and concentrated in regions of low ν. As the bloom intensifies P_{max} shifts towards higher values of ν, similar to the data (Figure 4).

From the analysis in Section 2.1 we know that bloom growth and intensity depends on the ratio α/γ (equation 8, Figure 3c). Namely, if α/γ is small – i.e. when the simulated death rate is small compared to the biological growth rate – $P(\nu)$ grows quickly in regions of low ν resulting in a more intense bloom, and if α/γ is large then $P(\nu)$ grows slowly at low ν. This is in agreement with the interpretation above regarding the rate at which chl-a grows at low SST (Figure 4). However, our model only considers a constant vertical mixing rate α for a single bloom whereas our interpretation of the data above suggests that the vertical mixing rate may change substantially as the bloom evolves.

We note that the variations in chl-a growth at low SST in the data could also be a result of changes in phytoplankton growth rate. This could be caused, for example, by variations in sunlight availability. This effect can be captured by varying γ in our model. Namely, if the early stage of the bloom in the data (Figure 4, blue) is experiencing a larger growth rate γ, this would be analogous to decreasing α/γ. Lower α/γ in turn leads to a steep bloom growth at low ν, or in the case of the data, low SST. Equivalently, the later bloom stage (red) may be experiencing a smaller growth rate, therefore increasing α/γ in the model and resulting in less steep bloom growth at low ν (SST).

4 Conclusions and Discussion

We have presented an idealized model with a number of paramaterized dynamical processes to investigate spatial and temporal characteristics of phytoplankton blooms at the sea-ice edge. This builds on work by Birch et al. (2007), using a modified version of the Fisher equation. Our model results suggest that ice edge blooms can be characterized by two distinct regimes: *(i)* Growth near the ice edge – as the phytoplankton are advected away from the sea-ice edge and confined to a meltwater-stratified shallow surface layer, their growth is determined by the ratio of biological growth rate to vertical mixing; *(ii)* Decay away from the ice edge – in regions beyond the peak bloom the phytoplankton concentration decreases together with the meltwater concentration, since a reduction in meltwater in the surface layer leads to weakened stratification and deeper vertical mixing of the plankton. Eventually, when the meltwater is well mixed the phytoplankton concentration returns to its background steady state levels present in the open-ocean.

The modeling results support a simple initiation mechanism for how meltwater helps drive algae spring blooms near the marginal ice zone: During the spring melt period, the marginal sea-ice zone features a highly stratified cold and fresh surface layer that is maintained by meltwater influx and populated with sea-ice algae. Constrained in the euphotic zone by the melt, the algae grow rapidly by photosynthesis into a phytoplankton bloom that peaks at a certain distance from the ice edge. This initiation mechanism suggests that blooms prosper in the stable environment provided by sea-ice meltwater and are dynamically impacted by meltwater concentration. The model developed here provides a framework to study the details of how these blooms evolve spatially and spread from near the ice edge to the open ocean over time.

Our framework assumes that the system is (at least initially) not nutrient limited, which can be the case early in the season after winter ice formation and corresponding brine rejection have driven vertical convection and enriched the ocean surface layer with nutrients. Ice edge blooms that occur later in the year may be substantially impacted by nutrient depletion as well as predation (Wassmann & Reigstad, 2011). We note that

the assumption of no nutrient limitation may hold better in Eastern Fram Strait – the region covered by the satellite scenes – than in other regions. In this region warm Atlantic Water is advected from the subtropics and may contain the nutrients needed to facilitate bloom development. This warm northward current can additionally drive the bloom as it also accelerates sea-ice melt (Randelhoff et al., 2018).

The hierarchical importance of phytoplankton blooms for a thriving ecosystem in the Arctic is a driving motivator to understand how their dynamics vary with current and future variations in sea-ice conditions. Under continued global warming, the spring sea ice edge is projected to retreat further and further north. This suggests that regions that currently experience large meltwater fluxes in the spring may lose this source of stratifying freshwater, and the focus of phytoplankton spring blooms will migrate to increasingly high latitudes. This may have far-reaching impacts on the Arctic ecosystem as a whole.

Acknowledgments

This work was supported by NSF OPP awards 1744835 and 1643445. Data used in this study (Landsat 8 scenes in Figure 1 and 4) were acquired via U.S. Geological Survey (USGS) Earth Explorer (https://earthexplorer.usgs.gov) and were processed using NASA SeaDAS (Baith et al., 2001). The authors thank Greenpeace for ship time and logistics support for the May 2019 field work during which this project was developed.

References

Arrigo, K. R., & van Dijken, G. L. (2015). Continued increases in arctic ocean primary production. *Progress in Oceanography*, *136*, 60–70.

Baith, K., Lindsay, R., Fu, G., & McClain, C. R. (2001). Data analysis system developed for ocean color satellite sensors. *Eos, Transactions American Geophysical Union*, *82*(18), 202–202.

Behrenfeld, M. J., & Boss, E. S. (2014). Resurrecting the ecological underpinnings of ocean plankton blooms.

Birch, D. A., Tsang, Y.-K., & Young, W. R. (2007). Bounding biomass in the fisher equation. *Physical Review E*, *75*(6), 066304.

Cherkasheva, A., Bracher, A., Melsheimer, C., Köberle, C., Gerdes, R., Nöthig, E.-M., ... Boetius, A. (2014). Influence of the physical environment on polar phytoplankton blooms: a case study in the fram strait. *Journal of Marine Systems*, *132*, 196–207.

Fisher, R. A. (1937). The wave of advance of advantageous genes. *Annals of eugenics*, *7*(4), 355–369.

Huisman, J., van Oostveen, P., & Weissing, F. J. (1999). Critical depth and critical turbulence: two different mechanisms for the development of phytoplankton blooms. *Limnology and oceanography*, *44*(7), 1781–1787.

Huppert, A., Blasius, B., & Stone, L. (2002). A model of phytoplankton blooms. *The American Naturalist*, *159*(2), 156–171.

Janout, M. A., Hölemann, J., Waite, A. M., Krumpen, T., von Appen, W.-J., & Martynov, F. (2016). Sea-ice retreat controls timing of summer plankton blooms in the eastern arctic ocean. *Geophysical Research Letters*, *43*(24), 12–493.

Jin, M., Deal, C., Wang, J., Alexander, V., Gradinger, R., Saitoh, S.-i., ... Stabeno, P. (2007). Ice-associated phytoplankton blooms in the southeastern bering sea. *Geophysical Research Letters*, *34*(6).

Kolmogorov, A., Petrovskii, I., & Piscunov, N. (1937). A study of the equation of diffusion with increase in the quantity of matter, and its application to a biological problem. *Byul. Moskovskogo Gos. Univ.*, *1*(6), 1–25.

Leu, E., Mundy, C., Assmy, P., Campbell, K., Gabrielsen, T., Gosselin, M., ... Gradinger, R. (2015). Arctic spring awakening–steering principles behind the phenology of vernal ice algal blooms. *Progress in Oceanography*, *139*, 151–170.

Lewis, K. M., van Dijken, G. L., & Arrigo, K. R. (2020). Changes in phytoplankton concentration now drive increased arctic ocean primary production. *Science*, *369*(6500), 198–202. Retrieved from `https://science.sciencemag.org/content/369/6500/198` doi: 10.1126/science.aay8380

Mahadevan, A., D'asaro, E., Lee, C., & Perry, M. J. (2012). Eddy-driven stratification initiates north atlantic spring phytoplankton blooms. *Science*, *337*(6090), 54–58.

Mayot, N., Matrai, P., Arjona, A., Bélanger, S., Marchese, C., Jaegler, T., ... Steele, M. (2020). Springtime export of arctic sea ice influences phytoplankton production in the greenland sea. *Journal of Geophysical Research: Oceans*, *125*(3), e2019JC015799.

Mayot, N., Matrai, P., Ellingsen, I., Steele, M., Johnson, K., Riser, S., & Swift, D. (2018). Assessing phytoplankton activities in the seasonal ice zone of the greenland sea over an annual cycle. *Journal of Geophysical Research: Oceans*, *123*(11), 8004–8025.

Mellard, J. P., Yoshiyama, K., Litchman, E., & Klausmeier, C. A. (2011). The vertical distribution of phytoplankton in stratified water columns. *Journal of theoretical biology*, *269*(1), 16–30.

NASA Goddard Space Flight Center, O. B. P. G., Ocean Ecology Laboratory. (2018 Reprocessing). *Moderate-resolution imaging spectroradiometer (modis) aqua chlorophyll data.* (Accessed on 06/23/2020) doi: data/10.5067/AQUA/MODIS/L3B/CHL/2018

Omand, M. M., D'Asaro, E. A., Lee, C. M., Perry, M. J., Briggs, N., Cetinić, I., & Mahadevan, A. (2015). Eddy-driven subduction exports particulate organic carbon from the spring bloom. *Science*, *348*(6231), 222–225.

Randelhoff, A., Reigstad, M., Chierici, M., Sundfjord, A., Ivanov, V., Cape, M., ... Kristiansen, S. (2018). Seasonality of the physical and biogeochemical hydrography in the inflow to the arctic ocean through fram strait. *Frontiers in Marine Science*, *5*, 224.

Sverdrup, H. (1953). On conditions for the vernal blooming of phytoplankton. *J. Cons. Int. Explor. Mer*, *18*(3), 287–295.

Taylor, A. (1988). Characteristic properties of models for the vertical distribution of phytoplankton under stratification. *Ecological modelling*, *40*(3-4), 175–199.

Taylor, J. R., & Ferrari, R. (2011). Ocean fronts trigger high latitude phytoplankton blooms. *Geophysical Research Letters*, *38*(23).

Truscott, J., & Brindley, J. (1994). Ocean plankton populations as excitable media. *Bulletin of Mathematical Biology*, *56*(5), 981–998.

Waniek, J. J., Holliday, N., Davidson, R., Brown, L., & Henson, S. (2005). Freshwater control of onset and species composition of greenland shelf spring bloom. *Marine Ecology Progress Series*, *288*, 45–57.

Wassmann, P., & Reigstad, M. (2011). Future arctic ocean seasonal ice zones and implications for pelagic-benthic coupling. *Oceanography*, *24*(3), 220–231.